WARWICK
THE UNIVERSITY OF WARWICK

Original citation:
Karamitaheri, Hossein and Neophytou, Neophytos. (2016) Phonon transport effects in one-dimensional width-modulated graphene nanoribbons. Journal of Applied Physics, 119 (24). 244302.

Permanent WRAP URL:
http://wrap.warwick.ac.uk/81311

Copyright and reuse:
The Warwick Research Archive Portal (WRAP) makes this work by researchers of the University of Warwick available open access under the following conditions. Copyright © and all moral rights to the version of the paper presented here belong to the individual author(s) and/or other copyright owners. To the extent reasonable and practicable the material made available in WRAP has been checked for eligibility before being made available.

Copies of full items can be used for personal research or study, educational, or not-for profit purposes without prior permission or charge. Provided that the authors, title and full bibliographic details are credited, a hyperlink and/or URL is given for the original metadata page and the content is not changed in any way.

Publisher's statement:
This article may be downloaded for personal use only. Any other use requires prior permission of the author and AIP Publishing.

The following article appeared in Karamitaheri, Hossein and Neophytou, Neophytos. (2016) Phonon transport effects in one-dimensional width-modulated graphene nanoribbons. Journal of Applied Physics, 119 (24). 244302. and may be found at http://dx.doi.org/10.1063/1.4954021

A note on versions:
The version presented here may differ from the published version or, version of record, if you wish to cite this item you are advised to consult the publisher's version.

For more information, please contact the WRAP Team at: wrap@warwick.ac.uk

go.warwick.ac.uk/lib-publications

Phonon transport effects in one-dimensional width-modulated graphene nanoribbons

Hossein Karamitaheri[1] and Neophytos Neophytou[2*]

[1]Department of Electrical Engineering, University of Kashan, Kashan 87317-53153, Iran

[2]School of Engineering, University of Warwick, Coventry, CV4 7AL, UK

[*]N.Neophytou@warwick.ac.uk

Abstract

We investigate the thermal conductance of one-dimensional periodic width-modulated graphene nanoribbons using lattice dynamics for the phonon spectrum and the Landauer formalism for phonon transport. We conduct a full investigation considering all relevant geometrical features, i.e. the various lengths and widths of the narrow and wide regions that form the channel. In all cases that we examine, we find that width-modulation suppresses the thermal conductance at values even up to ~70 % below those of the corresponding uniform narrow nanoribbon. We show that this can be explained by the fact that the phonon spectrum of the width-modulated channels acquires less dispersive bands with lower group velocities and several narrow bandgaps, which reduce the phonon transmission function significantly. The largest degradation in thermal conductance is determined by the geometry of the narrow regions. The geometry of the wider regions also influences thermal conductance, although modestly. Our results add to the ongoing efforts in understanding the details of phonon transport at the nanoscale, and our conclusions are generic and could also apply to other one-dimensional channel materials.

Keywords: low-dimensional phonons, graphene nanoribbons, thermal conductance, width-modulation, atomistic simulations, Landauer formalism, thermoelectrics.

I. Introduction

Heat transport in low-dimensional channels exhibits peculiar features which are not found in bulk materials and is recently raising significant interest for both fundamental research as well as technological applications. Examples of these features include that: i) the thermal conductivity could deviate from Fourier's law [1-5], ii) a crossover is observed from ballistic into diffusive transport regimes [6, 7], or from nano- to macro-scale behaviors [8, 9], iii) the thermal conductivity could even increase under channel width confinement [10, 11], iv) band mismatch under extreme confinement could result to phonon localization and 'effective transmission bandgaps' [12], v) heat transport could be below the Casimir or the amorphous limits, and many more [13, 14]. Several interesting device concepts have also emerged recently in the area of phononics, which attempt to use heat to perform transistor action [15], create heat rectifiers [16], engineer the sound velocities and phonon dispersions, etc. [13, 17, 18].

Regarding technological applications a significant amount of work related to phonon transport revolves around thermoelectricity, which requires materials with minimal thermal conductivities, but high electronic conductivities. A series of engineering techniques to reduce the thermal conductivity of nanoscale channels (without introducing severe disorder that will also reduce the electronic conductivity) are under investigation, i.e. the use of superlattice or superlattice-like geometries [19-22], engineering the surface roughness [23-26], the use of core-shell cross section modulated channels [27, 28], twinning superlattice channels [29], channel surface decoration and amorphization techniques, etc.

Another interesting recent idea to reduce the thermal conductivity without large channel distortion is the possibility of realizing periodic channel width-modulation to engineer the phonon bandstructure [8], but also simultaneously increase the power factor [30]. Xiong *et* al., for example, have investigated the thermal conductivity in twinning superlattice (SL) nanowires (zig-zag shaped material channels) using non-equilibrium molecular dynamics (NEMD) [29]. A specific configuration of the zig-zag geometry was found to minimize the thermal conductivity to 65% of the pristine nanowire value. A

complementary study was performed by Jiang *et* al. with very similar observations [31]. In a different study, Termentzidis *et* al. studied the effect of nano-constrictions on the thermal conductivity of SiC nanowires, again using NEMD [32]. Interestingly, they observed that the thermal conductivity of the diameter-modulated nanowires may be even smaller than that of a nanowire with a uniform narrow diameter (equal to that of the narrow region). They have attributed this to a significant thermal boundary resistance due to reflections of the low-frequency modes on the surfaces surrounding the constriction. In a more recent work, Blandre *et* al. have considered the amorphisation of the outer surface of diameter modulated Si nanowire channels, which resulted in even lower thermal conductivities [33]. Nika *et* al. have investigated the thermal conductivity of Si/Ge cross-section-modulated nanowires and found a large decrease in the thermal conductivity compared to the bulk material as well [27]. They attributed this to modifications of the phonon spectra in the modulated nanowires which 'reduces the group velocities and introduces localization of certain modes in both the narrow and the wider segments of the nanowire'.

In this work, we extend the investigation of the thermal conductivity of width-modulated channels to the graphene nanoribbon (GNR) channel. For this we employ lattice dynamics based on a force-field method and the Landauer formalism. Graphene and GNRs have huge thermal conductivities in their pristine form, reaching values as high as 3080-5150 W/mK at room temperature [9, 34-40]. Recent theoretical works even suggest values up to ~6000 W/mK, with a large proportion of phonon mean-free-paths beyond 10μm [41-43]. Previous works indicated that under certain conditions, GNR-based channels could provide very high thermoelectric performance as well [44, 45]. In addition, GNRs represent the most realistic 1D system available, and studies on this provide fundamental understanding on heat phonon in purely 1D systems. Other than considering a width-modulated GNR channel for the first time, we also perform an *exhaustive* investigation of the influence of the width-modulation geometry on the thermal conductivity, considering all relevant geometrical features, i.e. various lengths and widths of the narrow and wide regions that form the channel; which allows us to quantify the relative influence of each geometrical feature on the thermal conductivity. Quantitatively, in agreement with the studies in nanowire channels described above, we

also find that in all cases we examine, the thermal conductance is lower compared to the conductance of the uniform channel of width even equal to the *narrow* part of the channel. Surprisingly, however, we find features related to wave and/or ballistic natures of phonon transport, tht are more pronounced in graphene-based channels, and deviate from what one would expect under the particle and/or diffusive transport natures. Although channels with shorter periodicity consist of higher constriction density and intuitively they should experience larger thermal conductivity reductions, it is actually longer periodicity channels which suffer more, even when the more conductive wider region increases in length. Furthermore, although the wider part is less resistive, when its width surpasses the width of the narrow region by a couple of nanometers, any further increase does not affect thermal conductance. In fact, we are able to explain most observations by the fact that the phonon spectrum of the width-modulated channels undergoes severe band-folding, and thus it acquires less dispersive bands with lower group velocities and several narrow bandgaps, which reduce the phonon transmission function significantly.

The paper is organized as follows: In Section II we describe the models and methods we employ to calculate the phonon spectrum and phonon transport. In Section III we present the effect of width-modulation on the GNR phonon spectrum and transmission. Section IV presents a comprehensive study of all possible geometrical considerations and their influence on the thermal conductance – i.e. the effect of lengths L_n and L_w and widths W_n and W_w of the narrow and wide channel regions as shown in Fig. 1. Finally in Section V we summarize and conclude the work.

II. Methods

Under the harmonic approximation, the motion of atoms can be described by a dynamical matrix as:

$$D = [D_{3\times 3}^{(ij)}] = \left[\frac{1}{\sqrt{M_i M_j}} \begin{cases} D_{ij} & i \neq j \\ -\sum_{l \neq i} D_{il} & i = j \end{cases} \right] \quad (1)$$

where $M_{i,j}$ is the atomic mass of the i^{th}, j^{th} carbon atom (in this case all atoms have the same mass), and the dynamical matrix component between atoms 'i' and 'j' is given by:

$$D_{ij} = \begin{bmatrix} D_{xx}^{ij} & D_{xy}^{ij} & D_{xz}^{ij} \\ D_{yx}^{ij} & D_{yy}^{ij} & D_{yz}^{ij} \\ D_{zx}^{ij} & D_{zy}^{ij} & D_{zz}^{ij} \end{bmatrix} \tag{2}$$

where

$$D_{mn}^{ij} = \frac{\partial^2 U}{\partial r_m^i \partial r_n^j}, \qquad i, j \in N_A \text{ and } \quad m, n \in [x, y, z] \tag{3}$$

is the second derivative of the potential energy (U) after atoms 'i' and 'j' are slightly displaced along the m-axis and the n-axis (∂r_m^i and ∂r_n^j), respectively.

For setting up the dynamical matrix component between the i^{th} and the j^{th} carbon atoms, which are the N^{th} nearest-neighbors of each other, we use the force constant method (FCM), involving interactions up to the fourth nearest-neighbor. The force constant tensor is given by:

$$K_0^{(ij)} = \begin{bmatrix} \phi_r^{(N)} & 0 & 0 \\ 0 & \phi_{ti}^{(N)} & 0 \\ 0 & 0 & \phi_{to}^{(N)} \end{bmatrix} \tag{4}$$

where $\phi_r^{(N)}$, $\phi_{ti}^{(N)}$, and $\phi_{to}^{(N)}$ are the radial, the in-plane transverse, and the out-of-plane transverse components respectively. The force constant fitting parameters are taken from Ref. [46] and are shown to accurately reproduce the phonon dispersion of graphene. The 3x3 components of the dynamical matrix are then computed as:

$$D_{ij} = U_m^{-1} K_0^{(ij)} U_m \tag{5}$$

where U_m is a unitary rotation matrix defined as:

$$U_m = \begin{bmatrix} \cos\theta_{ij} & \sin\theta_{ij} & 0 \\ -\sin\theta_{ij} & \cos\theta_{ij} & 0 \\ 0 & 0 & 1 \end{bmatrix} \tag{6}$$

Assuming the graphene sheet is located in the x-y plane, θ_{ij} represents the angle between the x-axes and the bond between the i^{th} and j^{th} carbon atom.

The phonon dispersion can be computed by solving the following eigenvalue problem:

$$\left[D + \sum_{l} D_l \exp\left(i\vec{q}.\Delta\vec{R} \right) \right] \psi(\vec{q}) = \omega^2 \left(\vec{q} \right) \psi(\vec{q}) \qquad (7)$$

where D_l is the dynamical matrix representing the interaction between the unit cell and its neighboring unit cells separated by $\Delta\vec{R}$, and $\psi(\vec{q})$ is the phonon mode eigenfunction at wavevector $\vec{q}$.

The FCM is coupled to the Landauer approach for the calculation of the phonon transmission function and the lattice thermal conductance in the GNR. The Landauer method is appropriate for studies of phonon transport in periodic geometries. In the ballistic regime, the transmission probability of each subband is one, and therefore, the number of modes at each frequency represents the ballistic transmission function. Using the Landauer theory for phonon transport, the heat flow is proportional to the phonon transmission function $T_{\text{ph}}(\ )$, the Bose-Einstein distribution function $n(\ )$ of the two contacts, and the phonon energy/frequency as:

$$I_q = \frac{1}{h} \int_0 T_{\text{ph}}(\ ) \hbar \quad n_2(\ ) \quad n_1(\ ) \, d(\hbar\ ) \qquad (8)$$

The ballistic thermal conductance can then be calculated in the framework of the Landauer formalism as:

$$K_1 = \frac{1}{2\pi\hbar} \int_0^{\infty} T_{\text{ph}}(\omega) \hbar\omega \left(\frac{\partial n(\omega)}{\partial T} \right) d(\hbar\omega) \qquad (9)$$

where T is the temperature. In this work we consider room temperature T=300K. At room temperature and under ballistic conditions the function inside the integral spans the entire energy spectrum [10, 47], which allows phonons of all energies to contribute to the thermal conductance.

III. The effect of width-modulation on the phonon spectrum and transmission

Changes in the spectrum under channel width-modulation: We first examine the influence of channel width-modulation on the phonon spectrum of the GNRs. The phonon spectrum of the examined GNRs is shown in the sub-figures of Fig. 2. For clarity we only show the first 50meV out of the total 200meV of the phonon spectrum of the GNRs, which contributes the most to the thermal conductance. The colormap indicates the contribution of each phonon state to the phonon conductance (red indicating large and blue indicating small contribution). Figure 2a shows the phonon bandstructure of a uniform channel of width W = 1.35 nm, Fig. 2b shows a uniform narrower channel of width W = 0.61 nm, and Fig. 2c shows a width-modulated channel in which the widths of the wide and narrow regions are the same as the ones in Fig. 2a and Fig. 2b, respectively, i.e. W_w = 1.35 nm and W_n = 0.61 nm. The length of the two regions is equal to $L_w = L_n$ = 0.43 nm, as shown in the schematic of Fig. 2c. Comparing Fig. 2a and Fig. 2b, it is obvious that confinement results in reduction in the number of subbands in the spectrum, whereas the three acoustic modes still remain. Comparing Fig. 2a and Fig. 2b to Fig. 2c, however, it is evident that the bands soften throughout the entire spectrum, acquiring smaller slopes, and thus smaller phonon group velocities.

Figures 2d and 2e focus on the influence of the lengths of the narrow/wide parts of the width-modulated channel, L_n and L_w, respectively. Figure 2d shows the spectrum of the width-modulated channel as the length of the *narrow* part increases to L_n = 4.69 nm (~11 times the initial size shown in Fig. 2c). Figure 2e, on the other hand, shows the spectrum of the width-modulated channel as the length of the *wide* part increases to L_w = 3.87 nm (~9 times the initial size shown in Fig. 2c). We need to point out here that the geometries of the structures we employ contain very small feature sizes, which can be experimentally difficult to realize (although the armchair edges we use are shown to be stable [41, 48]). Our intention, however, is to provide fundamental understanding and information about the nature of phonon transport at the nanoscale in the presence of channel width-modulation and generic conclusions. These could possibly apply to other one-dimensional channel materials, or 'thicker' width-modulated materials which would be more stable and realizable. For example, semiconductor width-modulated nanowires were experimentally demonstrated and indicated no stability concerns [49, 50].

When the length of either region increases, the unit cell of the channel increases as well, which introduces more bands in the spectrum (more atoms in the unit cell results in more bands in the spectrum). The bands of these channels are folded because the unit cell is much larger than the unit cell of the original uniform GNR, but at the edge of the Brillouin zone the bands split, and acquire a lower slope. This makes the bands primarily more 'flat' compared to the bands of the uniform channels (either the wide or the narrow ones). As a consequence, a large number of *narrow bandgaps* appearsc in the phonon spectrum as the length of a region increases, in agreement with previous studies [19, 27, 29]. Both the appearance of bandgaps and the reduction in the group velocity, lead to reduction in the thermal conductance as we discuss below. This is evident in the cases of both geometries with long narrow constrictions, as in Fig. 2d, and geometries with long wide regions as in Fig. 2e. Below, we explicitly compute the changes in the group velocities of the major conducting bands (Fig. 3), and the narrow bandgaps in the transmission function (Fig. 4).

Changes in the group velocities of major bands with width-modulation: The phonon group velocities of the first three acoustic branches, the ZA, TA and LA bands, which are the major contributors to the thermal conductance (red-colored bands in Fig. 2), are shown in Fig. 3a, Fig. 3b and Fig. 3c, respectively. The dashed lines show the group velocities of these phonon modes in the uniform channels, the wider one with W = 1.35 nm and the narrower one with W=0.61nm as labeled in the sub-figures. The data points show the group velocities of these bands when width-modulation is introduced in the channel. The width-modulated channel considered has W_w = 1.35 nm and W_n = 0.61 nm. We keep the length of the wide parts of the channel L_w constant and increase the length of the narrow part of the channel L_n, i.e. corresponding to the situation where the structure shown in the schematic of Fig. 2c extends to that of Fig. 2d. The blue-dot lines show the cases for short wider regions L_W = 0.42 nm (as in the inset of Fig. 2d), whereas the red-cross lines show cases for channels with longer wider regions L_w = 3.83 nm (as in the schematic of Fig. 2e).

As a general observation, the group velocities of the dominant bands are in all cases lower than the velocities of at least one of the corresponding uniform channels,

either the narrow one or the wider one. Importantly, upon channel width-modulation, it is evident that the sound velocity of the dominant LA phonon branch (Fig. 2c) is lower compared to the velocities of *both* the uniform narrow and uniform wide corresponding channels. The fact that width-modulation softens more strongly the dominant LA mode, clearly indicates that it will also affect thermal conductance. For channels with long narrow regions, i.e. large L_n (right side of sub-figures), the group velocity approaches that of the uniform narrow channel, but as L_n decreases the group velocity also decreases, indicating the degrading effect in increasing constriction density as also mentioned in Ref. [23, 32, 33]. In the cases of the ZA and TA modes shown in Fig. 2a and 2b, respectively, the sound velocities also decrease upon increasing constriction density, but the reduction is less severe. The sound velocities remain in the intermediate region between those of the corresponding uniform narrow and wider channels, or slightly lower.

Phonon transmission function upon width-modulation: The second important effect of width-modulation, beyond reduced sound velocities, is the introduction of narrow bandgaps in the phonon spectrum. This strongly affects the phonon transmission function as illustrated in Fig. 4. Again, we compare the width-modulation channel with the corresponding uniform narrow/wide channels. The red lines in the sub-figures of Fig. 4a, 4b, and 4c show the phonon transmission versus phonon energy for the uniform wide channel with W_w = 1.35 nm, whereas the black lines show the transmission of the uniform narrow channel with W_n = 0.61 nm. The transmission of the uniform narrow GNR is lower across the spectrum compared to that of the uniform wider GNR, because of the smaller number of atoms in the unit cell, and therefore less phonon modes in the narrow channel. Figures 4a, 4b and 4c, include in addition the transmission of three width-modulated channels with different geometries as shown in the insets. In these examples we keep the widths of the wide and narrow regions constant at W_w = 1.35 nm and W_n = 0.61 nm and vary their lengths L_w and L_n.

In Fig. 4a the width-modulated channel has small periodicity with $L_n = L_w$= 0.43 nm (as shown in the inset) and the transmission is shown by the blue line. In Fig. 4b the width-modulated channel has elongated narrow regions with L_n = 4.69 nm and the

transmission is shown by the green line. In Fig. 4c the width-modulated channel has elongated wide regions with L_w = 4.69 nm and the transmission is shown by the magenta line. In all cases of width-modulated channels, it is evident that the transmission throughout the entire phonon spectrum is mostly below the transmissions of both the uniform wide channel (red line) and the uniform narrow channel (black line). Interestingly, a large number of oscillations and discontinuities are evident in the transmission features of the width-modulated GNRs, especially in Fig. 4b and 4c. These oscillations are the result of the large number of small bandgaps and band discontinuities that band-folding upon width-modulation introduces in the spectrum as shown in Fig. 2d and 2e.

The changes in the spectrum through the reduction of the group velocities and the introduction of narrow bandgaps, have a degrading effect on the thermal conductance. Figure 4d shows the cumulative thermal conductance of the channels under consideration as shown in Fig. 4a-4c. Clearly, the wider uniform channel with the largest amount of modes provides the highest thermal conductance (red line), followed by the uniform narrow channel (black line), despite the fact that this channel has the lowest number of modes. All width-modulated GNR channels have lower thermal conductances. The conductance of the GNR with small periodicity (or shorter narrow regions) is the largest (blue line), closely followed by the conductance of the channel with short narrow regions but larger wider regions (magenta line). The channel with the long narrow regions has the lowest thermal conductance (green line). Even constrictions placed at only a small part of the channel as in Fig. 4c, (i.e. a small constriction density), are detrimental to the thermal conductance (comparing the red with the magenta line). The thermal conductance drops even down to ~30% of the original value, in agreement with studies on Si nanowire diameter-modulated channels, where a 65% drop was reported upon diameter-modulation [32, 33].

It is also interesting to observe that the channels with short periodicity (blue lines in Fig. 4a and in Fig. 4d), in which the modulation appears more often along the length of the channel, have slightly higher thermal conductance than channels with larger periodicity in which case the modulation appears in larger intervals. The reason is that

channels with larger periodicity have larger unit cells, and undergo stronger band-folding, which results in many more narrow gaps in the spectrum in agreement with previous works [19, 27, 29, 51] (although not severely reduced group velocities as seen in Fig. 2). The large number of narrow gaps reduces the transmission and thermal conductance in channels with large periodicity. This is a result of band-folding in channels with larger unit cells, and it is an effect of the wave nature of phonons dominating transport. The trend would be reversed in channels where the wave (and ballistic) nature of transport is suppressed in favor of the particle (and/or diffusive) nature, as for example in channel materials with shorter phonon-phonon scattering mean-free-paths [33]. In that case, the channel can be thought of a series of resistances (where the constriction acts as an additional resistance). There, as the periodicity decreases, the constriction density increases, and thermal conductance drops. Similarly, as L_W increases, the overall thermal conductance would increase because the wide region is a less resistive region.

We mention here that 'transport' bandgaps appear even in uniform channels in the presence of surface roughness, which creates band mismatch and propagating modes cannot survive, and similarly they also reduce thermal conductance [12, 52]. That however, originates from disorder, whereas the bandgaps under width-modulation are actual bandstructure modifications. It is also worth noting that computing thermal conductance by directly using the phonon spectrum and phonon transmission (Fig. 2 and Fig. 4), allows for access to information about the transport of phonons at different energies, and the influence of effects such as band-folding and narrow bandgap formation becomes easily observed. This information might not be easily accessible when using other methods such as Monte Carlo or even Molecular Dynamics.

IV. Geometrical considerations of width-modulation feature sizes

Next we perform a comprehensive investigation of the thermal conductance of the width-modulated GNR by considering all geometrical features of the channel and its constrictions. We start by investigating the effect of the length of both the narrow and

wide regions L_n, and L_w, respectively, and then we perform an investigation for the effect of the widths of the narrow and wide regions W_n and W_w.

The effect of the lengths L_n and L_w on the thermal conductance: Figure 5 extends the results presented in Fig. 4 by considering the effect of increasing the *lengths* of the narrow and wide parts of the width-modulated channel independently. We keep the *widths* of these regions constant at W_w = 1.35 nm and W_n = 0.61 nm. The thermal conductances for GNRs of different L_w (length of wide region) spanning from L_w = 0.42 nm (blue line) to L_w = 3.83 nm (black line) are calculated, and plotted versus the length of the narrow region, L_n. The conductance of the corresponding uniform channels of width W_w = 1.35 nm and W_n = 0.61 nm are shown by the dotted lines and labelled accordingly. The important observation in this figure is that in all cases the phonon conductance of the width-modulated GNRs is lower than the conductances of both the uniform wide channel and the uniform narrow channel.

As intuitively expected, as the length of the narrow part L_n increases (at a constant L_w), the conductance drops. Interestingly, the conductance drops additionally by up to ~15% as the length of the wide region L_w increases (at a constant L_n) as well (i.e. blue versus black lines). This is counter intuitive, as one would have expected that the thermal conductance would have been the lowest in the structures with the highest constriction density, i.e. the shorter L_w, which increases the constriction resistance, as noted in Ref. [33] in the case of diameter-modulated Si nanowires. However, as explained above, increasing the periodicity of the channel increases the unit cell of the structure and results in a smaller Brillouin zone and enhanced band-folding with a large number of bands [27, 53]. Interaction between these different bands results in fragmented spectra with bands of lower group velocities and more narrow bandgaps, which reduce the thermal conductance. It is not surprising that solids with large unit cells with many atoms (small Brillouin zones), exhibit very low thermal conductivities.

Other works in the literature attempt to explain such effects in classical terms using simple phonon ray-tracing trajectories [24, 54]. In those terms, phonons could enter in regions where they can get trapped and undergo several reflections before they exit. In

our case, as L_w increases, phonons could more easily enter in the wide region of the channel and undergo multiple specular reflections which increase thermal resistance. When analyzing diameter-modulated Si nanowires, Sullivan *et* al. described how the specific geometry of the constrictions could form heat vortices in the wider regions, which impede the flow of phonons [23]. Thus, it seems that thermal conductance has a complicated behavior with regards to the exact geometry, the length scale of its features, the material, and probably the scattering mechanisms that dominate the nature of transport from wave to particle. The results of Ref. [33] for modulated Si nanowires, for example, which indicate a different trend for L_w variation, were computed in the presence of phonon-phonon scattering, which was not included in this study. The dominant mean-free-paths of phonon-phonon scattering in graphene and GNRs, however, are of the order of 100s of nanometers [55] which are much larger than in Si, and thus, we do not expect them to have significant influence on the length scales of the geometries we study, which are of the order of a few nanometers. Thus, we expect to have pronounced wave effects in phonon GNR transport, which increase the importance of band-folding, rather than summing up individual thermal resistances.

The thermal conductance values we present in Fig. 5, as well as in Fig. 7 and Fig. 8 below, are calculated under ballistic assumptions. They agree very well with literature values for the ballistic thermal conductance of graphene per unit cross section *A*, i.e. $K_{ball.}/A = 5.28 \text{ x } 10^9$ W/m^{2}K [55]. Indeed, using the conductance values of all the uniform channels we simulate, and assuming the GNR height to be 0.335nm, we reach $K_l/A = \left(3.61 \text{ to } 5.24\right) \text{ x } 10^9$ W/m^{2}K . The slightly lower values could originate from the changes in the graphene dispersion upon confinement in the GNR geometry. *The thermal conductivity* of the GNR channels, on the other hand, is a length dependent quantity and can be extracted using the thermal conductance and an estimate of the average phonon-phonon scattering mean-free-path (MFP) λ as $\kappa_l = \frac{K_l}{A}\frac{L\lambda}{(L+\lambda)}$ [56]. Values around λ ~700nm are very often found in the literature (although using a fixed value for the mean-free-path cannot capture the entire length dependence from the ballistic to the diffusive regimes). Nevertheless, if we use λ =775 nm from Ref. [57], width of *W*=4nm,

and length L=100μm (a length at which recent works claim that thermal conductance saturation is achieved in graphene [41-43]), then we can extract $\kappa_l = 2300$ W/mK, which is within the range of reported values. Mei *et* al., on the other hand, taking into account the energy dependence of the mean-free-paths within Monte Carlo simulations, reported that the more realistic saturation value could be much higher, closer to 6000 W/m-K, attributing this to their calculation that 20% of the phonon mean-free-paths are even larger than 100 μm [41]. The important point we would like to make, however, is that since the MFPs are so long, all experiments to date are performed in the ballistic or quasi-ballistic regime, and in such channel lengths our conclusions (which are based on the wave nature of transport) will be more valid and not influenced significantly by phonon-phonon scattering, thus wave effects are the ones which will dominate transport in these GNRs.

The effect of the narrow regions' width W_n on the thermal conductance: We now extend the analysis of the geometrical effects of the constrictions to focus on the influence of the width of the narrow region W_n on the thermal conductance, and afterwards on the effect of the width of the wide region W_w. Figure 6 demonstrates how the phonon spectrum changes upon changing/decreasing W_n. Figures 6a and 6b show the phonon spectrum of two uniform channels, a wide and a narrow channel of widths W_w = 4.06 nm and W_w = 0.40 nm, respectively (see schematics of Fig. 6a-b). Again, only the first 50 meV out of the 200 meV of the spectrum are shown for clarity. Comparing Fig. 6a to Fig. 6b, uniform width reduction reduces the number of modes in the spectrum. Figures 6c and 6d show the phonon spectrum in the presence of constrictions as the width W_n is reduced (see the middle part of the schematics). For the channel in Fig. 6c the constriction is small (with large W_n = 3.83 nm), and for the channel in Fig. 6d the constriction is large (with small W_n = 0.4 nm). The wide part of the channel has a constant width W_w = 4.06 nm. A comparison of Fig. 6a to 6c shows that the small constrictions introduced in Fig. 6c do not alter the phonon bandstructure noticeably. The large constrictions in Fig. 6d, however, alter the phonon spectrum significantly compared to both the corresponding uniform wide and narrow channels in Fig. 6a and 6b. The bands in Fig. 6d become much softer, and several narrow bandgaps appear in the spectrum,

evidence of coherent phonon scattering on the surfaces of the constrictions which becomes stronger as W_n decreases.

The thermal conductance of the GNR width-modulated channels as the width of the narrow region W_n changes (schematics of Fig. 6c and 6d), is shown in Fig. 7. Here, we consider channels of equal lengths for the narrow and wide regions i.e. $L_w = L_n$, but consider different lengths, spanning from 0.43 nm (blue line) to 1.7 nm (green line), as denoted in the figure. We keep the width of the wide parts of the channel constant at W_w = 4.06 nm in all cases, and examine how the thermal conductance changes as the width of the narrow region W_n changes. The dashed-dotted line shows the conductance of the corresponding uniform narrow channel of width $W = W_n$, which increases more or less linearly as expected. In the modulated channels, after a sharp initial drop when the constriction is introduced (right side of Fig. 7), the conductance decreases linearly with constriction width, W_n. This linear decrease was also observed in Monte Carlo simulations of much thicker width-modulated systems as well [58]. In that work, Zianni *et* al. define a quantity called 'transmissivity' which is just the geometrical ratio of the narrow over the wide part of the channel, $\mathrm{Tr} = W_n/W_w$, and they find a linear relationship between the thermal conductivity of the modulated channel and 'transmissivity' [58]. From Fig. 7, in our work the scaling of the conductance to the constriction geometry is larger than linear for large W_n, close to W_w, but becomes linear as W_n decreases. The more than linear drop in conductance for even very small width-modulation in our case is attributed to bandstructure effects such as band-folding and mini bandgap formation, which will not be present in Monte Carlo formalisms.

Importantly, however, for all width-modulated channels the phonon conductance is always lower than that of the corresponding uniform narrow channel. The slope of the conductance in Fig. 7 decreases and the drop at small width-modulations is larger as the lengths of the wide and narrow regions L_n and L_w increase, which again can be attributed to stronger band-folding. Thus, channels with a smaller unit cell (smaller periodicity – blue line) have larger conductance compared to channels with longer $L_n = L_w$ regions, despite the fact that the constriction density is higher.

The effect of the wide regions' width W_w on the thermal conductance: Finally, we examine the effect of the wide regions' width W_w on the thermal conductance. This is shown in Fig. 8. Here, we again consider channels of equal lengths for the narrow and wide regions $L_w = L_n$, and consider lengths spanning from 0.43 nm (blue line) to 1.7 nm (green line), as noted in the figure. We keep the width of the narrow part of the channel constant at $W_n = 1.35$ nm in all cases and examine how the thermal conductance changes as the width of the wide region W_w changes. Schematics 'A', 'B', 'C', and 'D' show the geometries of the GNRs under consideration, as labeled in Fig. 8. Schematic 'A' shows the uniform channel with $W_n = W_w = 1.35$ nm, and its thermal conductance is the highest as shown by the upper left data point in Fig. 8. As the wide part of the channel W_w increases (moving to the right), the thermal conductance drops. The drop is milder when the length of the regions L_w and L_n are short, i.e. moving from structure 'A' to 'B' (blue line), because of the smaller unit cell and the formation of fewer narrow bandgaps. In terms of classical trajectories as described in Ref. [24], phonons find it difficult to enter into very narrow regions (although if they do enter then they can become blocked). The thermal conductance drop is stronger when the length of the two regions L_n=L_w is larger, i.e. moving from structure 'A' to 'D' (green line) because of the stronger band-folding and more narrow bandgaps. Again, in terms of classical trajectories, a larger region allows more low-frequency phonons to enter and undergo multiple specular scattering events. Interestingly, however, in all cases, most of the conductance drop is observed at the initial stages when W_w begins to increase and the constriction begins to form (small differences between W_w and W_n are enough to reduce the conductance by a large amount). When the W_w increases beyond ~1 nm compared to W_n, the thermal conductance saturates, and no further reduction is observed. A possible explanation could be the fact that the constriction resistance, the introduction of small bandgaps, and the flattening of the bands in the spectrum, are mostly a consequence of an increase in the unit cell of the channel, which increases band-folding. An increase in the width of the wide region W_w does not increase the unit cell any further, and thus, it does not affect the constriction resistance which is already formed. This was also observed by Nika *et* al. [9] and Moore *et* al. [25]. Sullivan *et* al. using molecular dynamics in the case of Si nanowires in the presence of nano-constrictions, justified the irrelevance of large W_w on

the thermal conductance by explaining that the increase of the corrugation amplitude beyond a certain limit introduces atomic heat current separation between the corrugated ridges and the inner channel [23].

An important point that needs to be addressed, is that the edge details such as distortion, edge-roughness, non-perfect periodicity, as well as the orientation (AGNRs vs ZGNRs) could quantitatively affect the results shown. With regards to the edge orientation, we have also performed simulations for ZGNRs and recreated the data in Fig. 7 and Fig. 8 of the manuscript for AGNRs originally. These results are presented in the Appendix. The basic conclusion is that the effects we observe for AGNRs also appear in the case of ZGNRs. The amplitude of the thermal conductance, however, is slightly higher compared to that in AGNRs because, as we explain in Ref. [12], the dispersions in ZGNRs are more dispersive. With regards to the effect of distortion and non-perfect periodicity, which would be the more realistic scenario, Blandre *et* al. [33] considers width-modulated Si nanowires with amorphous outer shell regions of similar diameters as the GNR widths we consider. The thermal conductivity is even more drastically reduced due to the presence of the amorphous outer shell, which we suspect will happen for line-edge roughened GNRs as well.

V. Conclusions

In this work we investigated the thermal conductance of low-dimensional, ultra-narrow graphene nanoribbon (GNR) channels upon the presence of periodic modulation of the channel's width. We employed the force constant method for the description of the phonon modes and the Landauer approach for the calculation of phonon transmission. We presented an extensive investigation of the phonon spectrum features and thermal conductance in terms of all four geometrical features in the width-modulation channel, i.e. the lengths and widths of the narrow and wide regions that form the modulated channel. We showed that channel width-modulation causes a reduction in the thermal conductance to levels that are always lower by even up to ~70% compared to the

corresponding uniform *narrow* channels. Width-modulation increases the length of the channel's unit cell, which introduces band-folding. We show that this alters the phonon spectrum by softening the modes and reducing the corresponding phonon group velocities, but also by introducing several narrow bandgaps which result in a fragmented spectrum. These spectrum alterations result in transmission function reductions, and thus, thermal conductance reductions. We found that the drop in the conductance is predominantly determined by the width and length of the *narrow regions*. The thermal conductance experiences an almost linear drop as the width of the narrow region, W_n, is reduced. It continues to decrease as the length of the narrow region, L_n, increases, and eventually saturates at a value ~50% lower. An additional thermal conductance reduction is also observed, counter-intuitively, as the length of the wider region of the channel, L_w increases, although at a smaller degree. On the other hand, we show that the width of the wide region W_w, after a certain size, does not affect the thermal conductance significantly. To conclude, we note that the results presented in this work can be perceived as generic phonon transport features of 1D width-modulated channels, which could apply to other 1D channels beyond graphene nanoribbons. Such width-modulated channels could be useful for thermoelectric materials, which require ultra-low thermal conductivities. They point to a design direction which reduces the channel's thermal conductivity by surface engineering, rather than by introducing disorder in the bulk of the channel which would degrade the electronic properties as well.

APPENDIX: Simulation data for the zigzag-edge GNRs (ZGNRs)

Several studies have shown that armchair edge GNRs (AGNRs – the ones considerd in the main text) and zig-zag-GNRs (ZGNRs) differ in thermal conductivity [41, 59-62]. Thus, we find it instructive to present the corresponding simulation results as in Fig. 7 and Fig 8 in the main text, but for ZGNRs. The results are presented in Fig. A1(a) for the cases where the narrow part width W_n changes at a constant wide part width W_w and constant region lengths, L_n, and L_w, and Fig. A1(b) for the cases where the wider part width W_W changes at a constant narrow part width W_n. The basic conclusion is that the effects we observe for AGNRs also appear in the case of ZGNRs. The amplitude of the thermal conductance, however, is slightly higher compared to that in AGNRs because as we explain in Ref. [12] the dispersions in ZGNRs are more dispersive (dashed-green lines are for the ZGNRs, same data lines the green lines as in Fig. 7 and Fig. 8).

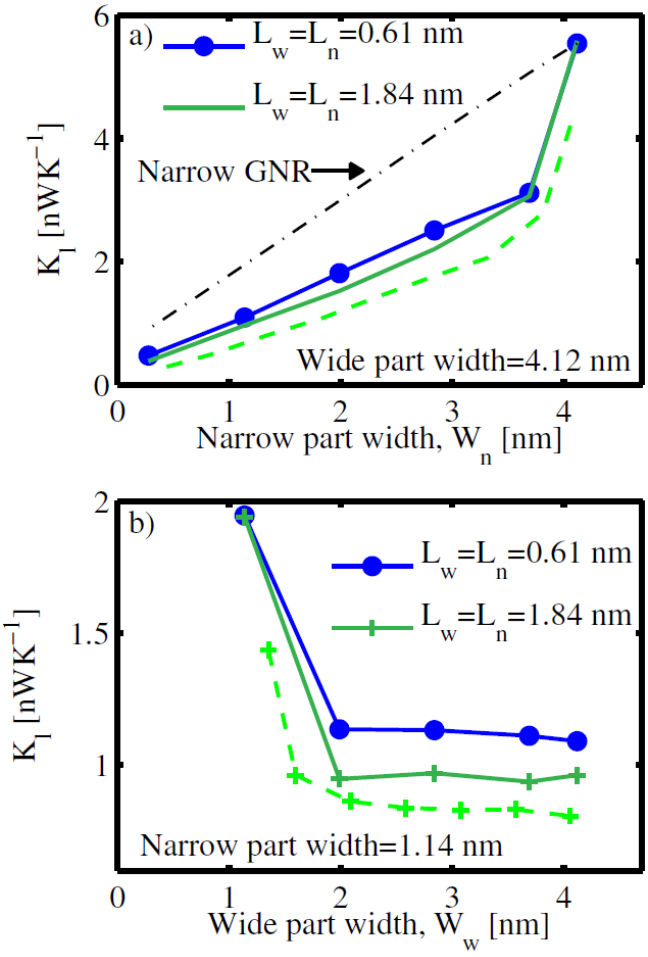

(a) The phonon conductance for width-modulated ZGNRs as the *width* of their narrow part, W_n, varies as in Fig. 7 in the main text (for AGNRs). Cases of ZGNRs with two different region lengths 0.61 nm (blue) and 1.84 nm (green) are shown; in both cases the wide and narrow region lengths are equal $L_w = L_n$. The wide part width is kept constant at W_w = 4.12 nm. The dashed-dotted line shows the conductance of the GNR channel with uniform width equal to W_n (x-axis values). As for AGNRs in Fig. 7, in all cases, the phonon conductance of the width-modulated ZGNRs is lower than that of the uniform channel of width equal to the narrow region's width W_n. The green-dashed line is the same as in Fig. 7 for AGNRs. (b) The phonon conductance for width-modulated ZGNRs as the wide part width W_w varies, as in Fig. 8 in the main text (for AGNRs). Again, cases of ZGNRs with two different region lengths 0.61 nm (blue) and 1.84 nm (green) are presented; in all cases the wide and narrow region lengths are equal $L_w = L_n$. The narrow part width is kept constant at W_n = 1.14 nm. In all cases, the phonon conductance is reduced as the wider part width W_w increases compared to the narrow part width W_n. Channels with smaller unit cell (smaller periodicity – blue line) have larger conductance. The conductance suffers significantly only initially as W_w increases and the constriction is formed. As the difference in W_n and W_w increases even more, no further reduction in conductance is observed. The green-dashed line is the same as in Fig. 8 (green line) for AGNRs.

References

[1] C. W. Chang, D. Okawa, H. Garcia, A. Majumdar, and A. Zettl, *Phys. Rev. Lett.*, 101, 075903, 2008.

[2] X. Ni, M. L. Leek, J.-S. Wang, and Y. P. Feng, B. Li, *Phys. Rev. B*, 83, 045408, 2011.

[3] Moran Wang, Nuo Yang, and Zeng-Yuan Guo, *J. Appl. Phys.*, 110, 064310, 2011.

[4] D. Singh, J. Y. Murthy, and T. S. Fisher, *J. Appl. Phys.*, 110, 113510, 2011.

[5] Z. Xu et al, *Nat. Comm.*, 5, 3689, 2014.

[6] S. Ghosh, W. Bao, D. L. Nika, S. Subrina, E. P. Pokatilov, C. N. Lau, and A. A. Balandin, *Nature Materials*, 9, 555-558, 2010.

[7] M. Bae, Z. Li, Z. Aksamija, P. N. Martin, F. Xiong, Z. Ong, I. Knezevic, and E. Pop, *Nat. Comm.* 4, 1734 (2013).

[8] A. I. Cocemasov, D. L. Nika, V. M. Fomin, D. Grimm, and O. G. Schmidt, Appl. Phys. Lett., 107, 011904, 2015.

[9] D. L. Nika, A. S. Askerov, and A. A. Balandin, *Nano Lett.*, 12, 3238-3244, 2012.

[10] H. Karamitaheri, N. Neophytou, and H. Kosina, *J. Appl. Phys.*, 115, 024302, 2014.

[11] D. Donadio and G. Galli, *Phys. Rev. Lett.*, 102, 195901, 2009.

[12] H. Karamitaheri, M. Pourfath, H. Kosina, and N. Neophytou, *Phys. Rev. B*, 91, 165410, 2015.

[13] E. Pop, *Nano Research*, 3, 147–169, 2010.

[14] P. G. Murphy and J. E. Moore, *Phys. Rev. B*, 76, 155313, 2007.

[15] P. B.-Abdallah and S.-A. Biehs, *Phys, Rev. Lett.*, 112, 044301, 2014.

[16] N. Yang, G. Zhang, and B. Li, *Appl. Phys. Lett.*, 93, 243111, 2008.

[17] M. Maldovan, *Nature*, 503, 209, 2013.

[18] S. P. Hepplestone and G. P. Srivastava, *Phys. Rev. B*, 84, 115326, 2011.

[19] T. Zhu and E. Ertekin, *Phys. Rev. B*, 90, 195209, 2014.

[20] A. Rajabpour and S. Volz, *Phys. Prev. B*, 90, 195444, 2014.

[21] Z.-X. Xie, K.-Q. Chen, and L.-M. Tang, *J. Appl. Phys.*, 110, 124321, 2011.

[22] Z. Aksamija and I. Knezevic, Phys. Rev. B, 88, 155318, 2013.

[23] S. E. Sullivan, K.-H. Lin, S. Avdoshenko, and A. Strachan, *Appl. Phys. Lett.*, 103, 243107, 2013.

[24] L. N. Maurer, Z. Aksamija, E. B. Ramayya, A. H. Davoody, and I. Knezevic, *Appl. Phys. Lett.*, 106, 133108, 2015.

[25] A. L. Moore, S. K. Saha, R. S. Prasher, and L. Shi, Appl. Phys. Lett., 93, 083112, 2008.

[26] P. N. Martin, Z. Aksamija, E. Pop, and Umberto Ravaioli, *Phys. Rev. Lett.*, 102, 125503, 2009.

[27] D. L. Nika, A. I. Cocemasov, D. V. Crismari, *Appl. Phys. Lett.*, 102, 213109, 2013.

[28] T. Markussen, *Nano Lett.*, 12, 4698-4704, 2012.

[29] S. Xiong, Y. A. Kosevich, K. Saaskilathi, Y. Ni, and S. Volz, *Phys. Rev. B*, 90, 195439, 2014

[30] X. Zianni, Appl. Phys. Lett., 97, 233106, 2010.

[31] J.-W. Jiang, N. Yang, B.-S. Wang, and T. Rabczuk, *Nano Lett.*, 13, 1670-1674, 2013.

[32] K. Termentzidis, T. Barreteau, Y. Ni, S. Merabia, X. Zianni, Y. Chalopin, P. Chantrenne, and S. Voltz, *Phys. Rev. B*, 87, 125410, 2013.

[33] E. Blandre, L. Chaput, S. Merabia, D. Lacroix, and K. Termentzidis, *Phys. Rev. B*, 91, 115404, 2015.

[34] N. Mingo, D. A. Broido, *Nano Lett.*, 5, 1221-1225, 2005.

[35] L. Lindsay, D. A. Broido, and N. Mingo, *Phys. Rev. B*, 80, 125407, 2009.

[36] L. Lindsay, D. A. Broido, and N. Mingo, *Phys. Rev. B*, 82, 115427, 2010.

[37] D. L. Nika and A. A. Balandin, *J. Phys.: Condens. Matter*, 24, 233203, 2012.

[38] A. Balandin, *Nat. Materials*, 10, 569, 2011.

[39] A. V. Savin, Y. S. Kivshar, and B. Hu, *Phys. Rev. B*, 82, 195422, 2010.

[40] Z. Aksamija and I. Knezevic, Phys. Rev. B., 90, 035419, 2014.

[41] S. Mei et al., J. Appl. Phys., 116, 164307, 2014.

[42] G. Fugallo et al. Nano Lett., 14, 6109, 2014.

[43] G. Barbarino et al., Phys. Rev. B, 91, 035416, 2015.

[44] H. Karamitaheri, N. Neophytou, M. Pourfath, R. Faez, and H. Kosina, *J. Appl. Phys.*, 111, 054501, 2012.

[45] F. Mazzamuto, V. H. Nguyen, Y. Apertet, C. Caer, C. Chassat, J. Saint-Martin, and P. Dollfus, *Phys. Rev. B*, 83, 235426, 2011.

[46] R. Saito, M. Dresselhaus, G. Dresselhaus, *'Physical Properties of Carbon Nanotubes'*, Imperial College Press, London, 1998.

[47] T. Markussen, A.-P. Jauho, and M. Brandbyge, Nano Lett., 8, 3771, 2008.

[48] P. Koskinen, S. Malola, and H. Hakkinen, *Phys. Rev. Lett.*, 101, 115502, 2008.

[49] G. D. Sulka, A. Brzózka, L. Liu, *Electrochimica Acta*, 56, 4972, 2011.

[50] S. K. Lim, S. Crawford, G. Haberfehlner, and S. Gradečak, *Nano Lett.*, 13, 331-336, 2013.

[51] D. L. Nika, E. P. Pokatilov, A. A. Balandin, V. M. Fomin, A. Rastelli, and O. G. Schmidt, *Phys. Rev. B*, 84, 165415, 2011.

[52] M. Luisier, *J. Appl. Phys.*, 110, 074510, 2011.

[53] E. Macia-Barber, *'Thermoelectric Materials – Advances and Applications,'* CRC Press, 2015.

[54] E. B. Ramayya, L. N. Maurer, A. H. Davoody, and I. Knezevic, Phys. Rev. B, 86, 115328, 2012.

[55] E. Munoz, J. Lu, and B. I. Yakobson, *Nano Lett.*, 2010, 10, 1652–1656.

[56] H. Karamitaheri, M. Pourfath, R. Faez, H. Kosina, IEEE Transactions on Electron Devices, 60, 2142, 2013.

[57] S. Ghosh, I. Calizo, D. Teweldebrahn, E. Pokatilov, D. Nika, A. Balandin, W. Bao, F. Miao, and C. Lau, Appl. Phys. Lett., vol. 92, pp. 151911-1–151911-3, May 2008

[58] X. Zianni, V. Jean, K. Termentzidis, and D. Lacroix, *Nanotechnology*, 25, 465402, 2014.

[59] Y. Xu et al., *Appl. Phys. Lett.*, 95, 233116, 2009.

[60] Z. W. Tan et al., *Nano Lett.*, 11, 214, 2011.

[61] Y. Wang et al., *Appl. Phys. Lett.*, 101, 013101, 2012.

[62] J. Wang et al., J. Phys.: Condens. Matter 24, 295403, 2012.

Figure 1:

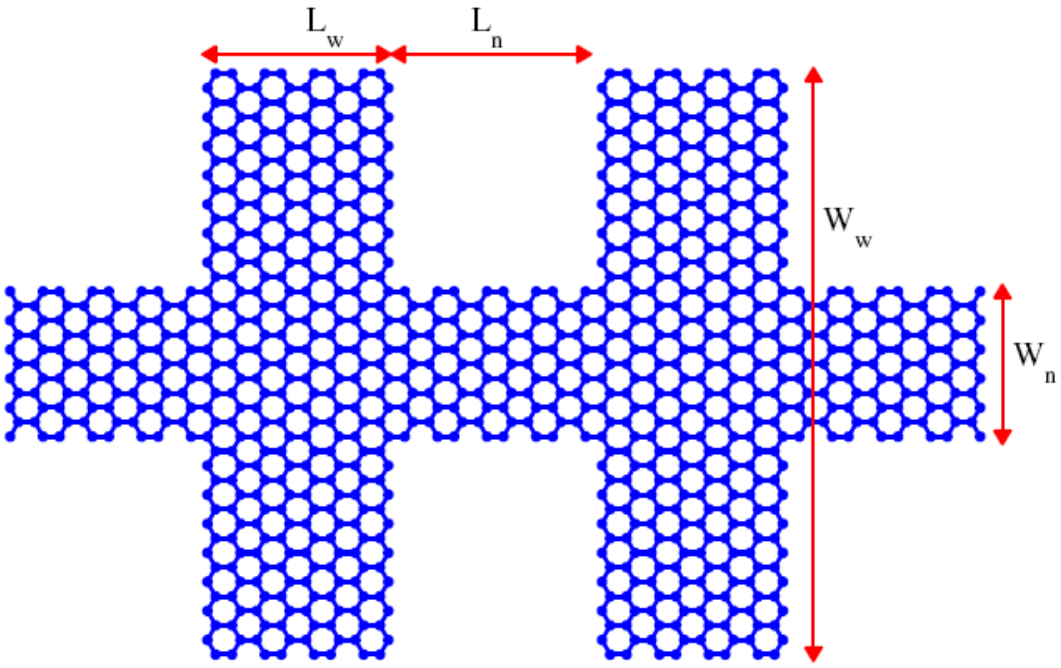

Figure 1 caption:

The modulated graphene nanoribbon geometry used in the simulations. The channel is periodic, and consists of wide regions of length L_w and width W_w, and narrow regions of length L_n and width W_n.

Figure 2:

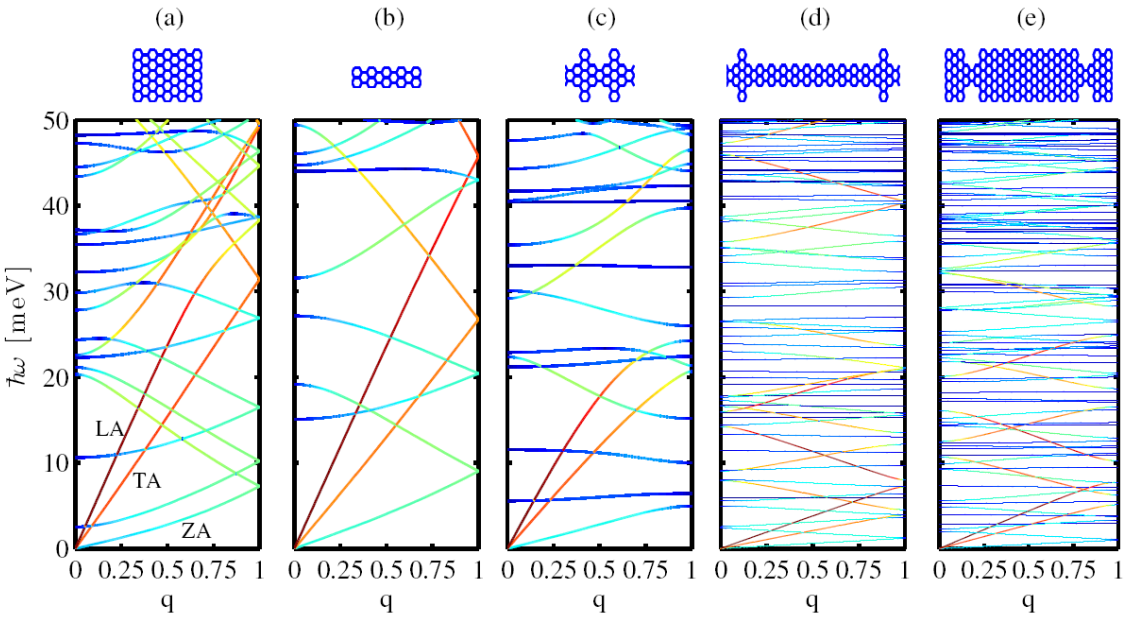

Figure 2 caption:

The effect of channel width-modulation on the phonon bandstructure of the GNRs with specific focus on the influence of the length of the wide/narrow parts, L_n and L_w. For clarity only the first 50 meV out of the 200 meV of the spectrum are shown. The wide part of the channel has width W_w = 1.35 nm, whereas the narrow part of the channel has width W_n = 0.61 nm. The phonon bandstructures of five different channels are presented: (a) A uniform wide channel with width W_w = 1.35 nm; (b) A uniform narrow channel with width W_n = 0.61 nm; (c) A width-modulated channel with equal wide and narrow region lengths L_w = L_n = 0.43 nm, as shown in the schematic; (d) A width-modulated channel with a short wide region but a longer narrow region i.e. L_w = 0.43 nm and L_n = 4.69 nm; (e) A width-modulated channel with a long wide region but a shorter narrow region i.e. L_w = 3.87 nm and L_n = 0.43 nm. The colormap indicates the contribution of each phonon state to the phonon conductance (red indicating large and blue indicating small contribution).

Figure 3:

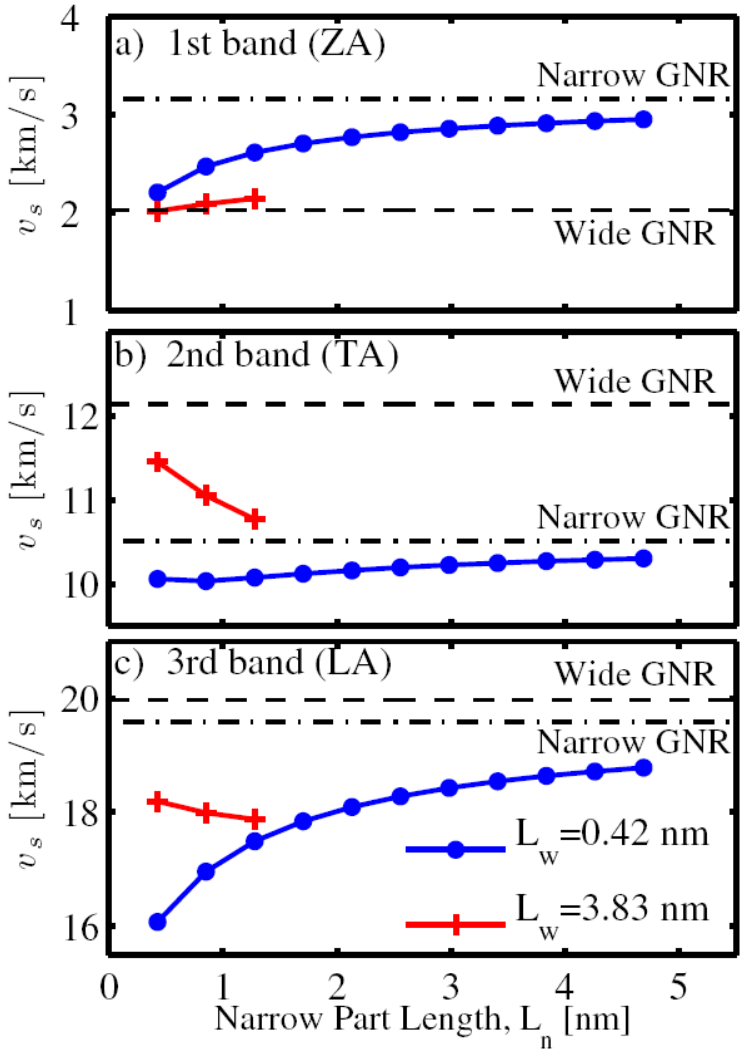

Figure 3 caption:

The bandstructure sound velocity of the first, second, and third phonon subbands (in (a), (b) and (c), respectively), for a width-modulated GNR channel with the width of the wide part being W_w = 1.35 nm and the width of the narrow part W_n = 0.61 nm. The sound velocities are plotted versus the length of the narrow part of the channel, L_n. Channel cases for which the length of the wide region is short at L_w = 0.42 nm (blue lines – channels as in the schematics of Fig. 2c, 2d) and longer at L_w = 3.83 nm (red lines – channel as in the schematic of Fig. 2e) are shown. The bandstructure velocities for the corresponding subbands of the uniform wide channel and the uniform narrow channel are indicated by the dashed lines and labelled accordingly.

Figure 4:

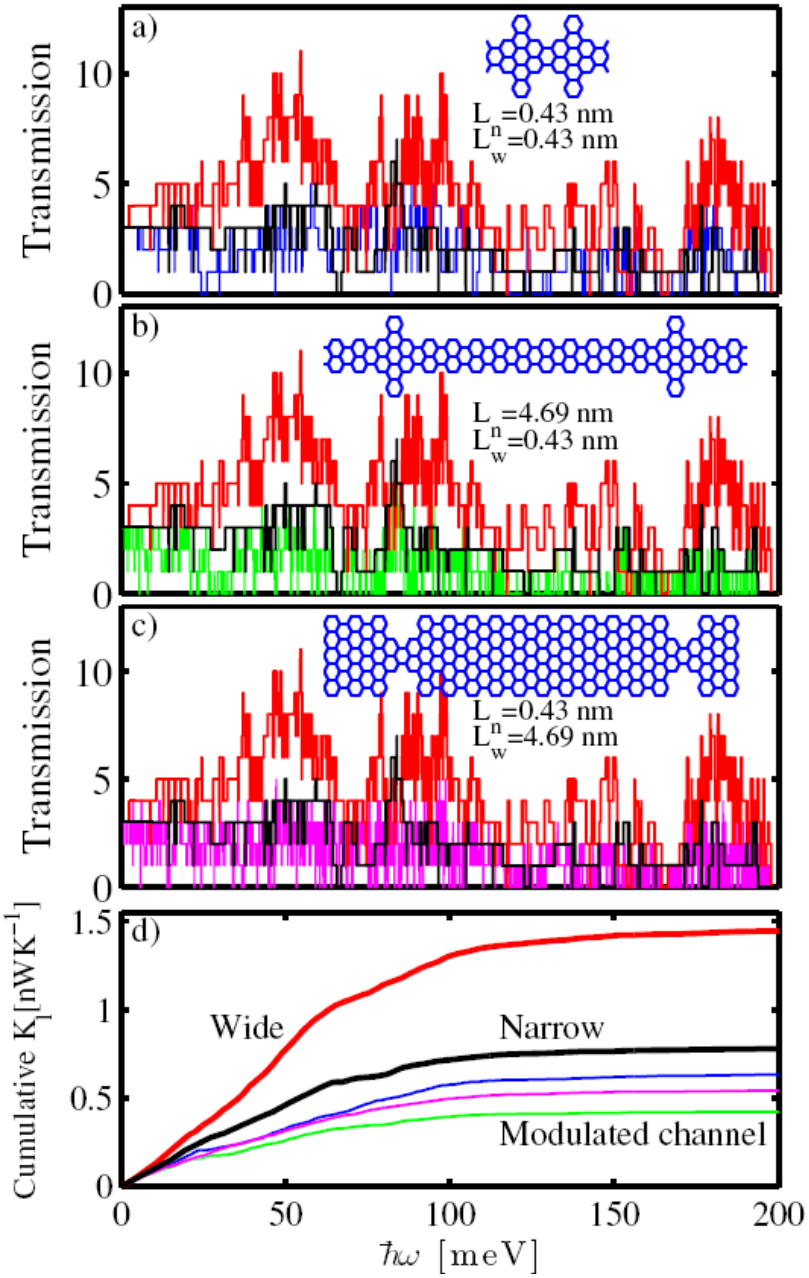

Figure 4 caption:

The effect of channel width-modulation on the GNR phonon transmission. The wide part of the channel has width W_w = 1.35 nm, whereas the narrow part of the channel has width W_n = 0.61 nm. Five different channel cases are presented. In all sub-figures the transmission of a uniform wide channel of width W = 1.35 nm is shown in red, whereas the transmission of a uniform narrow channel of width W = 0.61 nm is shown in black.

Additionally, in (a) the transmission of a width-modulated channel with equal wide and narrow region lengths $L_w = L_n = 0.43$ nm, as shown in the inset, is depicted in blue. In (b) the transmission of a width-modulated channel with a short wide region $L_w = 0.43$ nm, but longer narrow region $L_n = 4.69$ nm, as shown in the inset, is depicted in green. In (c) the transmission of a width-modulated channel with a long wide region $L_w = 3.87$ nm, but a shorter narrow region $L_n = 0.43$ nm, as shown in the inset, is depicted in magenta. (d) The cumulative conductance of these channels versus phonon energy.

Figure 5:

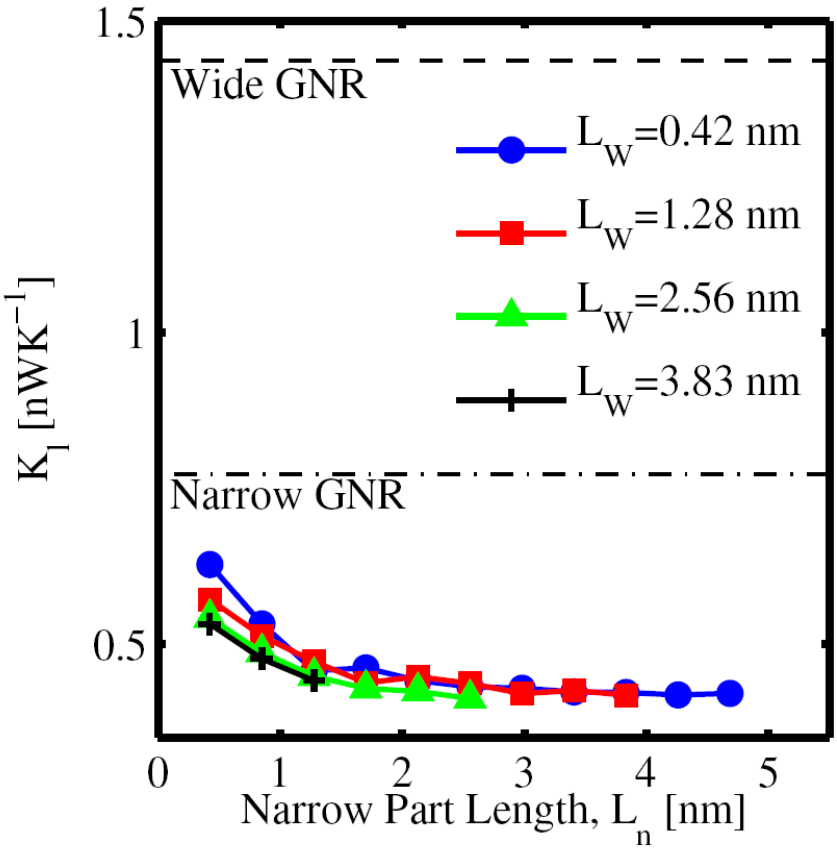

Figure 5 caption:

The thermal conductance of the width-modulated GNRs as the *lengths* of their narrow and wide regions L_n and L_w vary. Results for GNRs of different L_w spanning from 0.42 nm (blue) to 3.83 nm (black) are shown versus the length of the narrow region L_n. The width of the wide part is fixed at W_w = 1.35 nm and the width of the narrow part is fixed at W_n = 0.61 nm. The conductance of the corresponding uniform channels of widths W = 1.35 nm and W = 0.61 nm are shown by the dashed lines and labeled accordingly.

Figure 6:

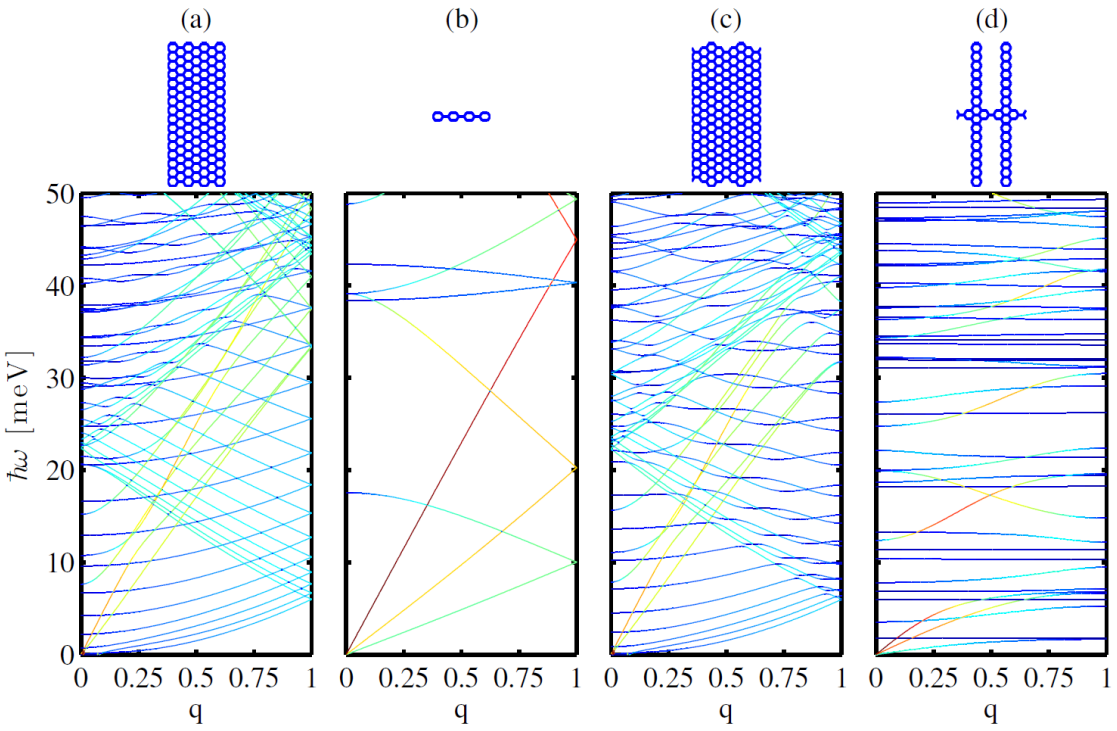

Figure 6 caption:

The effect of the GNR channel width-modulation on the GNR phonon bandstructure with specific focus on the influence of the width of the narrow region, W_n. For clarity only the first 50 meV out of the 200 meV of the spectrum are shown. The lengths of the regions are kept constant at $L_w = L_n = 0.43$ nm. The four sub-figures show the phonon spectrum of the channels in the schematics: (a) A uniform wide channel with width $W = 4.06$ nm; (b) A uniform narrow channel with width $W = 0.4$ nm; (c) A width-modulated channel with $W_w = 4.06$ nm and $W_n = 3.83$ nm (very small modulation); (d) A width-modulated channel with $W_w = 4.06$ nm and $W_n = 0.37$ nm (very large modulation); The colormap indicates the contribution of each phonon state to the phonon conductance (red indicating large and blue indicating small contribution).

Figure 7:

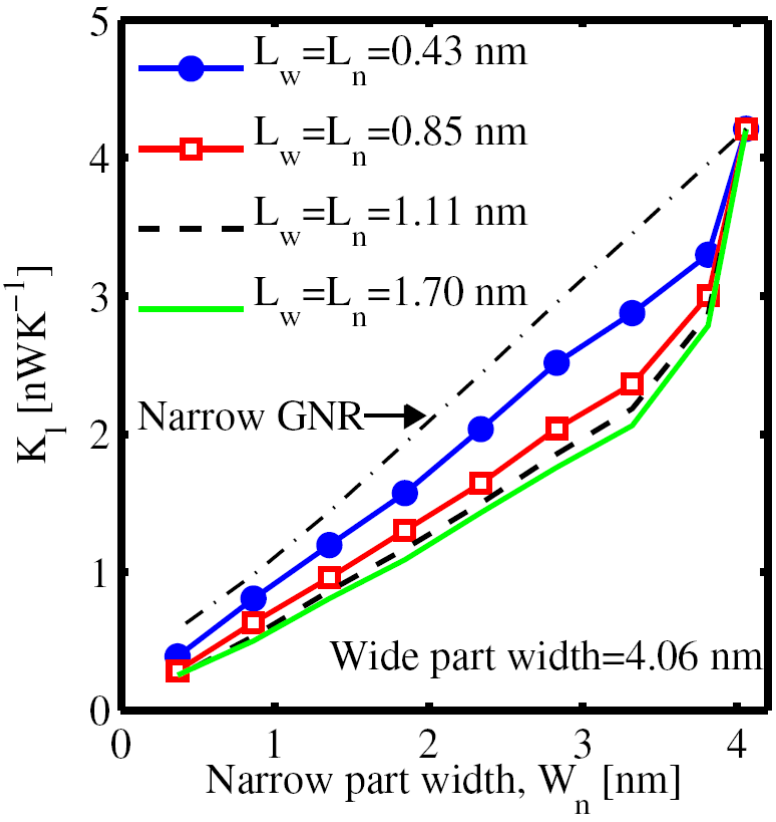

Figure 7 caption:

The phonon conductance for width-modulated GNRs as the *width* of their narrow part, W_n, varies. Cases of GNRs with different region lengths spanning from 0.43 nm (blue) to 1.70 nm (green) are shown; in all cases the wide and narrow region lengths are equal $L_w = L_n$. The wide part width is kept constant at $W_w = 4.06$ nm. In essence this figure shows the thermal conductance as the channel changes from what shown in the schematic of Fig. 6d to what is shown in the schematic of Fig. 6c. The dashed-dotted line shows the conductance of the GNR channel with uniform width equal to W_n (x-axis values), which increases linearly with W.

Figure 8:

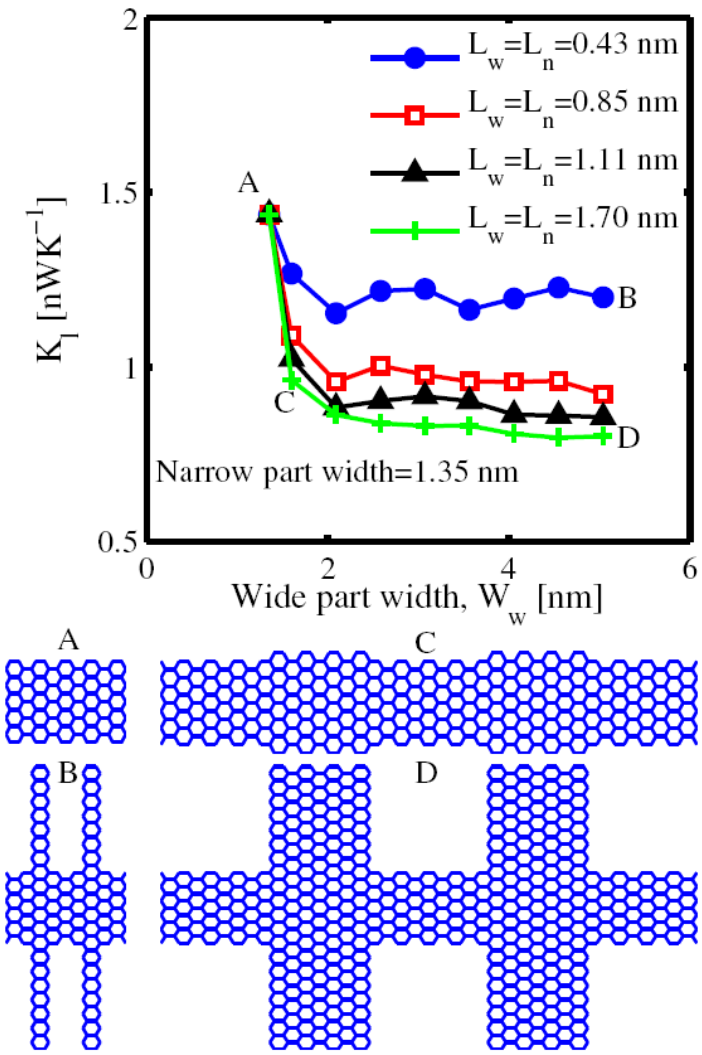

Figure 8 caption:

The phonon conductance for width-modulated GNRs as the wide part width W_w varies. Cases of GNRs with different region lengths spanning from 0.43 nm (blue) to 1.70 nm (green) are presented; in all cases the wide and narrow region lengths are equal $L_w = L_n$. The narrow part width is kept constant at W_n = 1.35 nm. Schematics 'A', 'B', 'C', and 'D' show the geometries of the GNRs under consideration as labeled in the figure.